Discover Oncology

RESEARCH Open Access

Stereotactic body radiation therapy (SBRT) increases anti-PD-1 antitumor activity by enhancing the tumor immune microenvironment in mice with metastatic hepatocellular carcinoma

Ke Xu[1,2†], Tao Gu[1†], Ke Su[1,3†], Xin Liu[1†], Bingsheng He[1], Jie He[1], Hao Chi[4], Xuancheng Zhou[4], Hanlin Liu[4], Rui Xiao[4], Xue Tang[4], Qinni Ye[4], Xue Zhou[1], Yingpeng Liu[1], Jie Xiong[5], Pan Wang[6], Han Li[1], Kun He[7,11*], Lu Guo[8*] and Yunwei Han[1,9,10,11*]

[†]Ke Xu, Tao Gu, Ke Su and Xin Liu have contributed equally to this work.

*Correspondence:
Kun He
hktongji@swmu.edu.cn
Lu Guo
guolu68@163.com
Yunwei Han
Lanpaoxiansheng@126.com

Full list of author information is available at the end of the article

Abstract

Background To explore the effect of radiotherapy on anti-pd-1 anti-tumor activity in metastatic hepatocellular carcinoma.

Methods Patients with metastatic HCC treated with intensity-modulated radiation therapy (IMRT) in combination with immunotherapy ($n=13$) were retrospectively analyzed by comparing its efficacy with that of immunotherapy alone ($n=12$) as well as untreated ($n=20$) patients with metastatic hepatocellular carcinoma. Animal experiment used mouse hepatocellular carcinoma H22 cell metastatic tumor model and were also divided into a control group, a PD-1 antibody group, an SBRT group, and an SBRT combined with a PD-1 antibody group. SBRT treatment is 8 Gy×3 F. The growth curves of body weight, irradiated tumor (the primary tumor), and non-irradiated tumor (secondary tumor) were plotted for each group of tumor-bearing mice. For this study, we used flow cytometry to examine effector CD8 + T cells expression in both irradiated and non-irradiated tumors, the CD4 + T and CD4+/CD8 + T cells ratio in the spleen, and used enzyme-linked immunosorbent assays (ELISA) to analyze the concentrations of IFN-γ and IL-10 in serum. Tumors were additionally stained with immunohistochemistry Ki-67 and TdT-mediated dUTP nick end labeling (TUNEL). We used hematoxylin-eosin (HE) staining of liver, spleen, lungs, kidneys, and heart to assess the anti-tumor activity of each group of tumor-bearing mice and their tolerance to determine the safety of the approach.

Results Clinical results: The median survival of IMRT + PD-1 group, PD-1 group, and control group were 17.5 months (95Confidence Interval (CI) 13.2–21.8), 12.5 months (95CI 9.0–16.0), and 5.2 months (95CI 5.5–12.9), respectively ($P<0.001$). SBRT combined with PD-1 antibody improved tumor control in both radiated and non-radiated tumors, resulting in a complete cure of the half of mice in animal studies. This was linked to an

increased in CD8 + effector T cells infiltration triggered by radiotherapy. HE staining of mice in the SBRT combined with the PD-1 treatment group suggested no damage to the liver, spleen, lungs, kidneys, and heart.

Conclusions This study showed that SBRT, while being well-tolerated, significantly increased anti-PD-1 antitumor activity by enhancing the tumor immune microenvironment in mice with metastatic hepatocellular carcinoma without significant toxic side effects.

Disclaimer : This manuscript was previously submitted as a preprint only in Experimental Hematology & Oncology and has no conflict of interest with this submission.

Keywords Stereotactic body radiation therapy, Tumor immune microenvironment, Immunotherapy, PD-1 antibody, Metastatic hepatocellular carcinoma, Toxic effects.

1 Introduction

Hepatocellular carcinoma (HCC) is one of the frequent primary liver cancers, responsible for almost 90% of all liver malignancies, according to the latest 2020 GLOBOCAN report. Indeed, in terms of its worldwide prevalence and death rates, primary liver cancer ranks sixth and third respectively [1]. HCC is a complex condition that has multiple etiologies including obesity, alcohol abuse, and chronic infections from hepatitis viruses. In fact, hepatitis B and C viruses remain a prominent risk factor for HCC progression, while non-alcoholic steatohepatitis, linked to diabetes or metabolic syndrome, has become a more prevalent risk factor in the West [2, 3]. This is because chronic viral infections can contribute to cirrhosis, a chronic liver disease preceding HCC and which occurs after prolonged inflammation and is followed by progression. This causes regenerative nodules and fibrotic tissues to replace healthy liver parenchyma, thereby leading to portal hypertension that creates a hypoxic environment conducive to tumor growth. The disease basically progresses from an asymptomatic stage (compensated cirrhosis) to a symptomatic one (decompensated cirrhosis), with subsequent complications generally linked to high mortality, decreased quality of life, and frequent hospitalization [4, 5]. The risk of hepatocellular carcinoma due to immune dysfunction occurs with cirrhosis formation and increases as liver function impairment progresses [6].

The incidence and fatality rates of hepatocellular carcinoma are steadily rising. Early-stage HCC is treated surgically, whereas more advanced HCC is treated with surgery combined with chemotherapy [7–10]. For the early-stage HCC, in addition to surgery, liver transplantation, and local ablation therapy can result in an overall survival rate of >60%. In contrast, advanced HCC treated with chemoembolization or systemic therapy tend to be less effective [11, 12]. However, most individuals with hepatocellular carcinoma are already in late stages when diagnosed [13]. The FDA has authorized the medicine sorafenib as the first-line treatment for HCC patients, showing 13.6 months of median survival [14]. Compared to sorafenib, lenvatinib is another first-line therapeutic option for advanced HCC, however, it did not enhance the survival rate for the unadjusted cohort (HR: 0.85, 95% CI 0.70–1.02) [15]. In recent years, the ESMO clinical practice guideline states that regorafenib and cabozantinib have recently been approved by FDA as second-line therapy for patients with advanced HCC whose disease had progressed after first-line treatment [3].

A new cancer treatment i.e., immunotherapy to regulate and destroy tumor cells by reducing the suppressed condition in the tumor microenvironment of immune cells and activating the body's own immune system. In numerous types of cancer, immune checkpoint modulators (represented by anti-CTLA4 and anti-PD-1/PD-L1 antibodies) have shown surprising anti-tumor effects, thus ushering in a new era of cancer treatment. There are many kinds of immune checkpoint receptors in hepatocellular carcinoma, among which CTLA-4, PD1, PD-L1/2, LAG-3, TIM-3 and TIGIT are deeply studied (Fig. 4). The McAbs of the corresponding five receptors have been successfully developed, and some of them have been approved by FDA, which has benefited patients a lot [16]. Compared with conventional therapies, immunotherapy has become a hot topic in basic and clinical cancer research as it enhances immune function, delays tumor progression and inhibits tumor recurrence and metastasis, and prolongs patient survival [17–19].

Additionally, radiation treatment at one tumor site has been observed to regression of metastatic cancer in a distant unirradiated site, with this effect known as the"abscopal effect" [20, 21]. This effect is associated with mechanisms involving the immune system and can be mediated through its activation [22]. Radiation can enhance the immunogenicity of tumors by promoting the release and presentation of tumor neoantigens, altering the immunogenicity of the tumor microenvironment (TME), as well as enhancing the recruitment and activation of effector T cells [23]. T cell infiltration or survival/proliferation of pre-existing T cells may be boosted and radiotherapy [24]. The main effector molecule secreted by these tumor infiltrating lymphocyte (TIL) is IFN-γ, which inhibits tumor cell growth [25]. TME includes a variety of suppressive immune cells, including Treg cells, which accumulate in the tumor microenvironment and secrete the cytokine IL-10, which inhibits activation of effector T cells [26]. However, this effect is rare because existing immune tolerance mechanisms may preclude the development of a sufficiently potent"abscopal effect"at treatment time [20]. Radiation therapy for advanced hepatocellular carcinoma has gained a lot of interest for improving the effectiveness of immunotherapy, because of its abscopal compartmentalization effect [27]. For solid tumors, Stereotactic body radiation therapy (SBRT), a novel kind of radiation treatment that delivers higher doses to smaller target lesions, has been shown to have potential anti-cancer benefits by greatly boosting local and distant control and improving survival [28]. However, the immunogenic effects of these radiations are also more pronounced, causing them to promote vascular destruction and exacerbate tumor hypoxia. In contrast, anti-PD-1 therapy not only leads to tumor regression but also reduces tumor hypoxia [29].

Hence, an increasing body of evidence suggests that radiation therapy combined with immunotherapy may be used to treat both local and metastatic diseases that can reduce the risk of"abscopal effect" [20, 30]. Induction of immunogenic cell death, enhancement of neoantigen expression and presentation, and CD8 + T cell activation and infiltration provide preclinical rationale for combined radiation and immune checkpoint blockade (ICB) approach [31]. Therefore, the current research aimed to explore the effect of radiotherapy on anti-PD-1 activity in metastatic hepatocellular carcinoma. Its tolerability and toxicity were also evaluated to guide clinical applications.

2 Materials and methods

2.1 Clinical information

This retrospective analysis involved three groups of BCLC-B/C HCC patients namely those who were untreated (control group), those who received PD-1 inhibitor monotherapy, and those who were given intensity-modulated radiotherapy (IMRT) along with PD-1 inhibitors from September 2018 to January 2022 at the Affiliated Hospital of Southwestern Medical University. IMRT (48 Gy) was performed during the first cycle of PD-1 inhibitors therapy (including Tislelizumab, Sintilimab, Camrelizumab, and Pembrolizumab) within 7 days of treatment and the major objective of the study was on overall survival (OS) for patients. This trial complied with the Declaration of Helsinki and was approved by the Clinical Trials Ethics Committee of the Affiliated Hospital of Southwest Medical University (Approval No. KY2020254). Due to the retrospective nature of the study, the requirement for informed consent was waived by the Ethics Committee of the Affiliated Hospital of Southwest Medical University. No potentially identifying information or images of human participants are included in this article.

Inclusion criteria were as follows: (1) There are more than 2 liver tumors in cytological or clinical diagnosis; (2) age ≥ 18 years old; (3) Eastern US Cancer Cooperation Group (ECOGPS) expression status 0–1; (4) no severe major organ dysfunction; (5) tumor clearly visible on at least one CT or MR diagnostic image; (6) BCLC stage: B-C (Intermediate and advanced); (7) The patients are treatment-naive. The exclusion criteria were as follows: (1) pacemakers, additional implants, or transportable electronic medical equipment; (2) any severe physical or mental illness; and (3) insufficient information.

2.2 Experimental materials

Mouse-derived hepatocellular carcinoma H22 cells were purchased from Purisel Life Sciences Ltd (Wuhan, China) while KM mice were purchased from Speford Biotechnology Ltd (Beijing, China). Fetal bovine serum, penicillin, and RPMI1640 culture medium were purchased from Invesco Jieji Trading Ltd (Shanghai, China). IvVivoPlus anti-mouse PD-1 for injection was obtained from BioXcell (USA) while CD3+, CD4+, and CD8 + antibodies were also purchased from Sporicon Biotechnology Ltd (Chengdu, China). CD45 + antibody was purchased from Thermo Fisher Scientific (USA). TdT-mediated dUTP nick end labeling (TUNEL) kits, Ki-67 antibody, and enzyme-linked immunosorbent assays (Elisa) kits were obtained from Wuhan Service Biotechnology Ltd (Wuhan, China). A purification process was not necessary since all of the chemicals were of analytical grade.

2.3 Cell culture

Cell culture was performed in 25 cm^2 cell culture flasks by adding H22, at a density of 10^6 cells/ml, to 5 ml of RPMI1640 culture medium containing 10% of fetal bovine serum as well as 1% of penicillin/streptomycin. This was followed by incubation under 5% CO_2 at 37 °C. Cells grown to 80% confluence were then used for cell passaging and subsequent experiments.

2.4 Animal model

Cultured H22 cells were first collected to prepare a cell suspension of 1×10^7 cells/ml in RPMI1640 medium. Six- to eight-weeks old male KM mice of weight 18–20 g were then

selected and each mouse was subcutaneously injected with 1×10^6 cells in the left lower limb. The tumor formation reached 100% after about 1 week. Three days after the first inoculation of H22 cells in the left lower limb, the process was repeated with the right lower limb. After tumor formation, tumor sizes were then measured every three days, with treatment starting when the diameter of the left lower limb tumor (primary tumor) reached approximately 7 mm. In this case, radiation therapy was used on the left lower limb tumor (primary tumor) while the right lower limb one (secondary tumor) received no radiation. The size of the tumors did not exceed 3000 mm^3 as required by the Animal Ethics Committee of Southwest Medical University.

2.5 Tumor treatment

The experimental groups in this study included a control, a PD-1 antibody group, an SBRT group, and an SBRT combined with a PD-1 antibody group, each containing 12 mice. No therapeutic intervention was applied to the control while mice were given intraperitoneal injections of murine-derived PD-1 antibody for the PD-1 antibody group, at a dose of 200 μg per mouse every three days for four times; Mice in the SBRT group were irradiated with a linear gas pedal (Varian Medical Systems, Inc, USA) at a dose of 8 Gy and a dose rate of 300 cGy/min for 3 days. For the last group, irradiation was coupled with murine-derived PD-1 antibody at a dose of 200 μg per mouse by intraperitoneal injection once every 3 days for 4 times. The volumes of primary and secondary tumors were measured every three days during the treatment (volume = ½×length×$width^2$). Moreover, four mice from each group were randomly on the 17th day of therapy, and their blood was extracted for ELISA analysis of IL-10 and IFN-γ concentrations in serum. For further investigation, flow cytometry was used to examine both primary and secondary tumors CD8 + T, and the CD4 + and CD8 + T cells in the spleen. Hematoxylin-eosin (HE) staining of the spleen, liver, kidney, lung, and heart was also used to assess the toxicity and overall anti-tumor effectiveness. Immunohistochemical Ki-67 and TUNEL staining, and Tumor debridement of primary and secondary tumors were performed on randomly selected four mice in each group, and Image J software was used for Ki-67 and TUNEL staining quantitative analysis results. However, the remaining 4 mice in each group were utilized to observe the tumor size with the naked eye. To examine the survival cycle of mice, the body mass weight curves and tumor growth curves of various groups of tumor-bearing mice were also plotted. Animal experiments were carried out in accordance with animal care guidelines and were authorized by the Institutional Animal Care and Treatment Committee of Southwest Medical University (Luzhou, China) (approval No. SWMU20220042).

2.6 Flow cytometry and enzyme-linked immunosorbent assay (ELISA)

Mouse tumors and spleens were obtained, and both were cut into small pieces. Tumors were then digested with type IV collagenase (1 mg/ml), hyaluronidase (1%), and DNAase I (0.25%) at room temperature for about 0.5 h, washed thrice with PBS, they were filtered through a 300-mesh screen and centrifuged at 300 g for 5 min to obtain tumor-infiltrated single nucleated cells. After cell counting, the antibodies CD45+, CD3+, CD4+, and CD8 + were added to the corresponding flow tubes and protected from light at 4 °C for 30 min prior to detection. However, the spleen was placed on a 300-mesh metal mesh, ground with PBS, and filtered into a 15 mL centrifuge tube. The supernatant was poured off after

centrifugation at 300 g for 5 min, and cells were resuspended in 3 mL of erythrocyte lysis solution, Lysis was then performed for 10 min at 37 °C before being terminated with 10 mL PBS, centrifugation at 300 g for 5 min, and the cell precipitate was retained. PBS solution was used to resuspend cells, which were then filtered through a 300-mesh sieve. To obtain splenic single nucleated cells, the cells were resuspended in PBS solution and filtered through a 300-mesh sieve. The CD8 + T effector cells expression were observed in the tumor as well as CD4 + T cells and CD4+/CD8 + T cells in the spleen.

After obtaining whole blood specimens from each group of tumor-bearing mice, it was kept for 2 h at room temperature before being centrifuged at 3000 rpm for 15 min at 2–8 ℃. The resulting supernatant was then used for the assay. For the ELISA, a standard curve was prepared based on the concentration and optical density (OD) value of the standards, and the concentrations of IFN-γ and IL-10 in the samples were subsequently determined from the standard curve.

2.7 Immunohistochemical Ki-67 and TUNEL staining

We used 10% neutral formalin to fix the tumor cells tissues for 24 hours, transferred it to 70% ethanol, and sliced it up into 4-μm-thick sections. The terminal deoxynucleotidyl transferase-dUTP nick end labeling (TUNEL) and Ki-67 were used to stain the tumor section, respectively. A microscopic examination was performed and images were acquired for analysis. Paraffin section immunohistochemistry Ki-67 results were interpreted as follows: hematoxylin-stained cell nuclei were blue, and positive expression, revealed by 3,3'-diaminobenzidine (DAB), was brownish-yellow. For the paraffin section white light TUNEL, results could be interpreted as follows: DAPI-stained nuclei were blue under UV excitation, the kit was FITC fluorescein-labeled, and positive apoptotic nuclei were brownish-yellow. Image J software was used for quantitative analysis of TUNEL and Ki-67 staining results.

2.8 Hematoxylin-eosin (HE) staining

All of the primary organs (liver, spleen, lungs, kidneys, and heart) were fixed in 10% neutral formalin solution for 24 h before being transferred to 70% ethanol and embedded in paraffin wax before being cut into 4-μm-thick pieces. Paraffin sections of specimens were dewaxed prior to staining with hematoxylin-eosin (HE). The sections were then sealed with neutral treacle. Microscopic examination (Nikon, Japan), image acquisition, and analysis were performed. The nuclei were dyed blue, while the cytoplasm was dyed red for the HE staining process.

2.9 Statistical analyses

All statistical analyses were performed using SPSS 26.0, while box and line plots with errors were generated using GraphPad Prism 8.0 (GraphPad Software, La Jolla, CA).

Basic patient characteristics were described using frequencies and percentages. For numerical variables, tests for normality were performed with the Kolmogorov-Smirnova method and the Shapiro-Wilk method of normality. Chi-square between groups was also tested using the Levene chi-square test. Normally- and non-normally-distributed numerical variables were then provided as mean ± standard deviation and median (P25, P75) respectively. To estimate the median survival of the survival data, the Kaplan-Meier curves were used.

Comparisons of composition ratios between groups (three IMRT + anti-PD-1 groups, anti-PD-1 group, and untreated group) were executed via the chi-square test for patient baseline characteristics; comparisons of OS between patient groups were performed using the Log-Rank method; Normally-distributed numeric variables and chi-squares were analyzed using one-way ANOVA or the non-parametric Kruskal-Wallis test as required; comparisons of tumor volume growth trends between groups were performed using Repeated measures ANOVA was used for the comparison of tumor volume growth trend between groups. Two-by-two comparisons were corrected by the Bonferroni method. The statistical significance was defined as $p < 0.05$.

3 Result

3.1 Comparison of clinical efficacy of radiotherapy combined with immunotherapy

Forty-five HCC patients (IMRT + anti-PD-1 group, 13; anti-PD-1 group, 12; untreated group, 20) were enrolled in the study between September 2018 and January 2022. Table 1 provides an overview of the patients' baseline characteristics. As of May 2022, the median survival was 17.5 months (95% CI 13.2–21.8),12.5 months (95% CI 9.0–16.0) and 5.2 months (95CI 5.5–12.9) for the IMRT + anti-PD-1, anti-PD-1 and control respectively ($P < 0.001$). Furthermore, compared with the control, both IMRT + anti-PD-1 and anti-PD-1 groups had significantly prolonged OS ($P < 0.001$, $P = 0.009$). This difference was not statistically significant between IMRT + anti-PD-1 group and anti-PD-1 group ($P = 0.191$), even though the IMRT + anti-PD-1 group had longer OS than the anti-PD-1 group (Fig. 1). After multivariate analysis, age ($P = 0.032$) and treatment ($P < 0.001$) were the two factors affecting OS (Table 2).

3.2 SBRT combined with PD-1 antibody enhances the apparent curative effect in mice

A schematic diagram of the treatment regimen using H22 cells to construct a model of tumor-bearing mice is shown in Fig. 2A. Better tumor control was observed in primary and secondary tumors when SBRT was coupled with the PD-1 antibody. Significant ($P < 0.001$) tumor suppression in SBRT coupled PD-1 antibody group vs. anti-PD-1 group ($P < 0.001$), and tumor suppression in SBRT coupled PD-1 antibody group vs. SBRT group ($P = 0.001$) of primary tumors were shown in Fig. 2B. SBRT coupled to PD-1 antibody group vs. Control group for Secondary tumor ($P < 0.001$), SBRT coupled PD-1 antibody group vs. anti-PD-1 group tumor suppression was significant ($P < 0.05$, $P = 0.013$), and SBRT coupled with PD-1 antibody group vs. SBRT group tumor suppression was significant ($P < 0.001$) as shown in Fig. 2C. To visualize the tumor growth, H22 tumor-bearing mice were euthanized 17 days after treatment, with pictures taken after stripping the primary and secondary tumors as shown in Fig. 2D-E. Among them, there was a 6/12 abscopal effect in the group of tumor-bearing mice who had SBRT with PD-1 antibody. According to the results, tumor control may have been improved with the combined treatment.

3.3 SBRT combined with PD-1 antibody treatment significantly enhanced systemic immune response

Compared with the other groups, tumor-bearing mice that were treated with SBRT coupled to PD-1 antibody had significantly more CD8 + effector T cells. Two-by-two comparisons with Bonferroni correction further showed that, for primary tumors,

Table 1 Baseline characteristics

Variable	IMRT + anti-PD-1	anti-PD-1	Control	P
Patients	13	12	20	
Male sex	11 (84.6)	10 (83.3)	18 (90.0)	0.837
Age ≥ 60 years	5 (38.5)	5 (41.7)	11 (55.0)	0.597
Child–Pugh				0.111
A	10 (76.9)	7 (58.3)	8 (40.0)	
B	3 (23.1)	5 (41.7)	12 (60.0)	
Number of tumors ≥ 2	11 (84.6)	10 (83.3)	18 (90.0)	0.837
Tumor diameter, cm				0.457
< 5	3 (23.1)	2 (16.7)	1 (5.0)	
≥ 5, < 10	7 (53.8)	5 (41.7)	13 (65.0)	
≥ 10	3 (23.1)	5 (41.7)	6 (30.0)	
Serum AFP, ng/ml				0.12
< 400	8 (61.5)	4 (33.3)	14 (70.0)	
≥ 400	5 (38.5)	8 (66.7)	6 (30.0)	
BCLC stage				0.944
B	3 (23.1)	3 (25.0)	4 (20.0)	
C	10 (76.9)	9 (75.0)	16 (80.0)	
HBV	9 (69.2)	7 (58.3)	10 (50.0)	0.55
Portal vein invasion	10 (76.9)	7 (58.3)	12 (60.0)	0.535
Lymph node metastasis	3 (23.1)	4 (33.3)	6 (30.0)	0.843
Extrahepatic metastases	2 (15.4)	2 (16.7)	4 (20.0)	0.938
Lung	1 (7.7)	2 (16.7)	2 (10.0)	
Bone	1 (7.7)	0	3 (15.0)	
PD-1 inhibitor type				0.864
Camrelizumab	4 (30.8)	5 (41.7)	0	
Pembrolizumab	2 (15.4)	2 (16.7)	0	
Sintilimab	4 (30.8)	2 (16.7)	0	
Tislelizumab	3 (23.1)	3 (25.0)	0	

IMRT: intensity modulated radiation therapy; PD-1: programmed cell death-1; HBV: hepatitis B virus; BCLC: Barcelona Clinic Liver Cancer; AFP: alpha fetoprotein

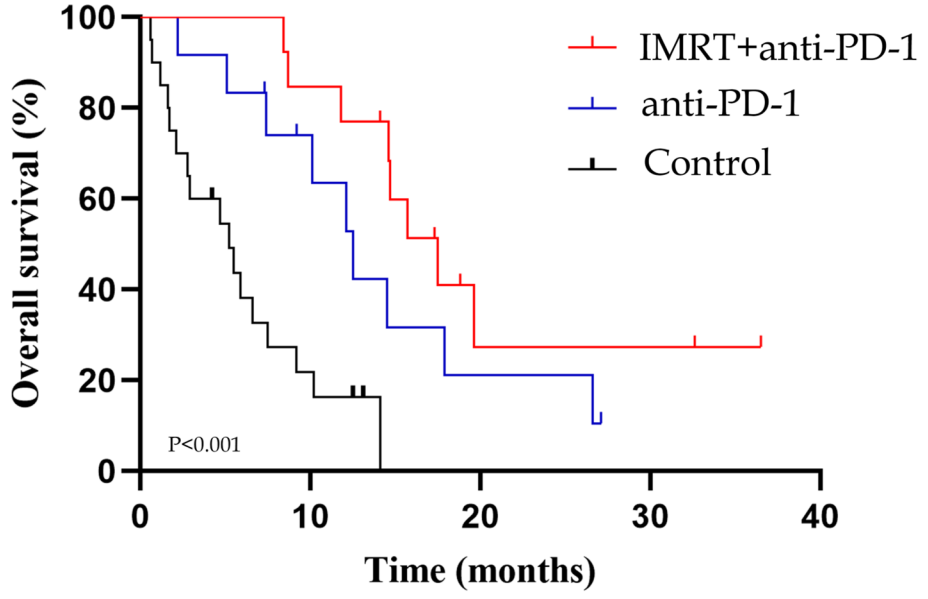

Fig. 1 Overall survival curve for IMRT plus anti-PD-1 group, anti-PD-1 group, and control group. IMRT + anti-PD-1, anti-PD-1 and control ($P < 0.001$). control vs. IMRT + anti-PD-1 ($P < 0.001$). control vs. anti-PD-1 ($P = 0.009$). IMRT + anti-PD-1 vs. anti-PD-1 ($P = 0.191$)

Table 2 Univariate and multivariate cox regression analyses for overall survival

Variable	Univariable cox regression			Multivariable cox regression		
	HR	95%CI	*P*	HR	95%CI	*P*
Sex (male/female)	1.027	0.397–2.660	0.867			
Age (≥ 60/<60 years)	0.444	0.224–0.882	0.02	0.445	0.213–0.931	0.032
Child-Pugh class (B/A)	2.482	1.233–4.997	0.011	1.682	0.793–3.571	0.175
Number of tumor (≥ 2/<2)	0.834	0.321–2.170	0.71			
Tumor diameter (≥ 5/<5 cm)	2.615	0.782–8.748	0.119			
AFP (≥ 400/<400 ng/ml)	0.656	0.328–1.316	0.235			
BCLC stage (B/C)	0.64	0.265–1.548	0.322			
HBV (positive/negative)	0.549	0.276–1.095	0.089			
Portal vein invasion (yes/no)	0.826	0.408–1.674	0.596			
Lymph node metastasis (yes/no)	0.807	0.384–1.695	0.571			
Extrahepatic metastases (yes/no)	1.766	0.764–4.084	0.183			
Treatment			< 0.001			< 0.001
None	1			1		
RT + immunotherapy	0.134	0.049–0.362	< 0.001	0.124	0.044–0.352	< 0.001
Immunotherapy	0.247	0.097–0.627	0.003	0.236	0.091–0.615	0.003

AFP, alpha fetoprotein; BCLC, Barcelona Clinic Liver Cancer; HBV, hepatitis B virus; RT, radiation therapy.

combining SBRT with PD-1 antibody significantly increased CD8 + effector T cells compared with the control ($P < 0.001$) or the anti-PD-1 group ($P < 0.001$). SBRT combined with PD-1 antibody group vs. CD8 + effector T cells in SBRT group ($P < 0.001$) are shown in Fig. 3A-B. SBRT coupled PD-1 antibody group vs. CD8 + effector T cells in Control group for Secondary tumor ($P < 0.001$), SBRT combined with PD-1 antibody group vs. anti-PD-1 group for CD8 + effector T cells ($P < 0.01$, $P = 0.0044$), and SBRT coupled PD-1 antibody group vs. SBRT group for CD8 + effector T cells ($P < 0.01$, $P = 0.0011$) are shown in Fig. 3C-D. The spleen was studied by flow analysis, and CD4 + T cells were significantly elevated in the SBRT combined with PD-1 antibody group vs. Control group ($P < 0.001$), SBRT combined with PD-1 antibody group vs. anti-PD-1 group ($P = 0.001$), and SBRT combined with PD-1 antibody group vs. SBRT group ($P < 0.01$, $P = 0.0035$) as shown in Fig. 3E-F. After analyzing the ratio of CD4+/CD8 + T cells in spleen samples, it was observed that CD4+/CD8 + T cells were significantly elevated in the SBRT combined with the PD-1 antibody group compared with the control ($P < 0.001$), or the anti-PD-1 group ($P < 0.01$, $P = 0.0069$). CD4+/CD8 + T cells were significantly elevated in the SBRT combined with PD-1 antibody group vs. SBRT group ($P < 0.01$, $P = 0.0049$) as shown in Fig. 3G. The concentration of IFN-γ in serum samples from each group of tumor-bearing mice was analyzed by ELISA, it was found to be significantly elevated in the SBRT combined with the PD-1 antibody group compared with the control group ($P < 0.001$), the anti-PD-1 group ($P < 0.001$) and the SBRT group ($P < 0.001$) as shown in Fig. 3H. In addition, the changes in IL-10 concentrations in serum samples were analyzed, with the concentrations being significantly lower after the combination therapy in comparison with the control group ($P < 0.001$), the anti-PD-1 group ($P < 0.01$, $P = 0.0015$), and the SBRT group ($P < 0.001$) as shown in Fig. 3I. In conclusion, these results suggest that SBRT increased anti-PD-1 activity by enhancing the tumor immune microenvironment in mice.

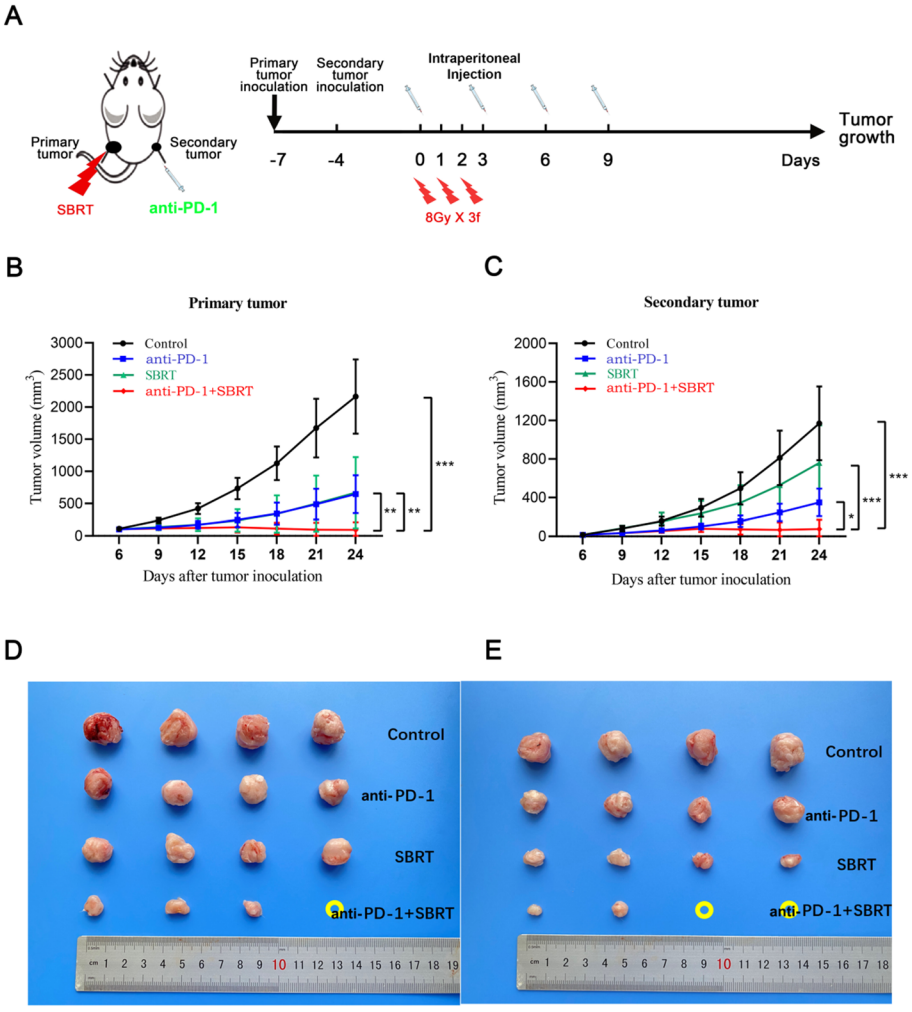

Fig. 2 SBRT combined with PD-1 antibody treatment enhances tumor control in tumor-bearing mice. **A** Treatment protocol. **B** Primary tumor growth curve of tumor-bearing mice ($n = 12$ mice/group, 2-way analysis of variance for tumor growth). The tumor curves of SBRT group and PD-1 antibody group overlap in the figure. **C** Secondary tumor growth curve of tumor-bearing mice ($n = 12$ mice/group, 2-way analysis of variance for tumor growth). **D** Mice in each group were stripped of Primary tumor on day 17 after treatment ($n = 4$ mice/group). **E** Isolation of Secondary tumor in each group of mice on day 17 after treatment ($n = 4$ mice/group). (Yellow circles in the tumor solid figure represent tumor regression). ($^{*}P < 0.05$. $^{**}P < 0.01$. $^{***}P < 0.001$)

3.4 Decreased proliferation and increased apoptosis after combining SBRT with PD-1 antibody

Primary and secondary tumors of each group were subjected to immunohistochemical Ki-67 assay, and pictures, as obtained by pathology section scanner (P250 Flash 3DHISTECH), are shown in Fig. 4A. The immunohistochemical Ki-67 values of primary and secondary tumors in each group were analyzed by ImageJ software, and the results were consistent with normality and chi-square, using a one-way method. Figure 4B shows the Ki-67 values for SBRT combined with PD-1 antibody group compared with the control group in the primary tumor ($P < 0.001$), Ki-67 values in SBRT combined with PD-1 antibody group vs. anti-PD-1 group ($P < 0.01$, $P = 0.007$), Ki-67 values in SBRT combined with PD-1 antibody group vs. SBRT group ($P < 0.05$, $P = 0.049$). Figure 4C shows the Ki-67 values in SBRT combined with PD-1 antibody group vs. Control group for secondary tumor ($P < 0.001$), SBRT combined with PD-1 antibody group vs.

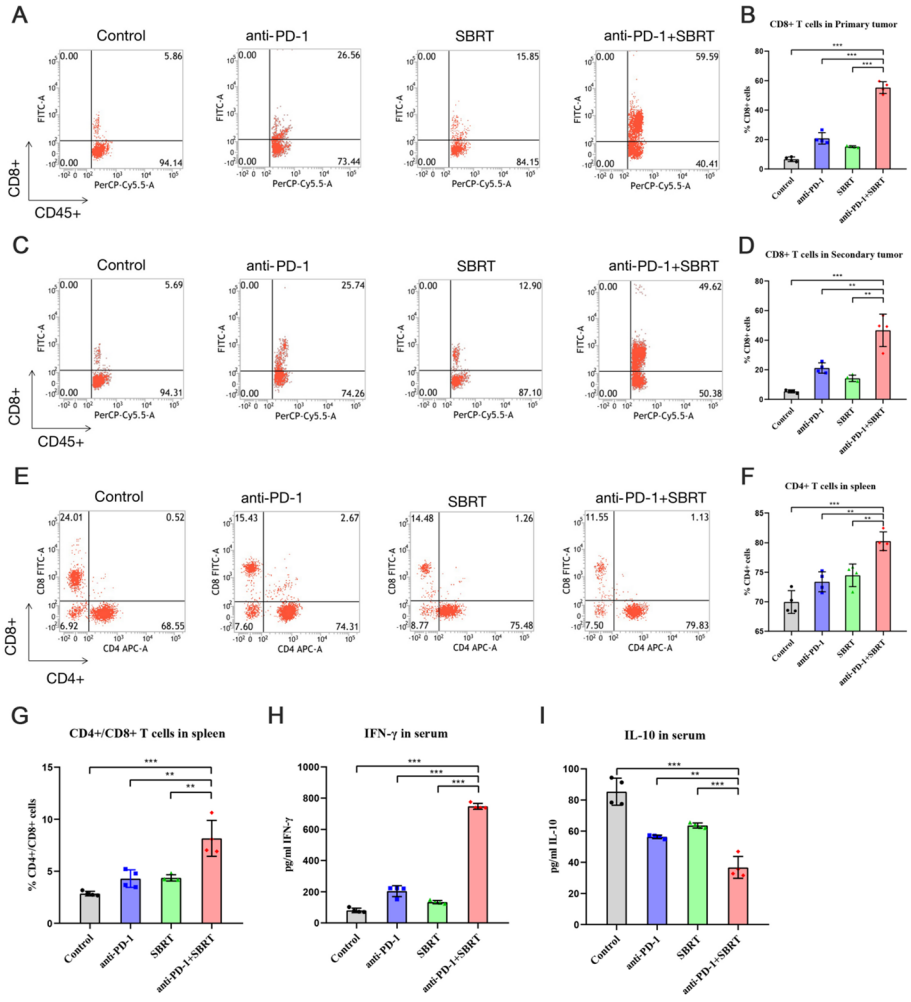

Fig. 3 SBRT combined with PD-1 antibody treatment significantly enhanced the systemic immune response. **A** Flow cytometry staining of primary tumor in each group of tumor-bearing mice 17 days after initiating treatment. **B** Quantification of the percentage of CD8 + effector T cells in primary tumor 17 days after initiating treatment ($n = 4$ mice/group, one-way ANOVA). **C** Flow cytometry staining of secondary tumor in each group of tumor-bearing mice 17 days after initiating treatment. **D** Quantification of the percentage of CD8 + effector T cells in secondary tumor 17 days after initiating treatment ($n = 4$ mice/group, one-way ANOVA). **E** Flow cytometry staining of spleens from each group of tumor-bearing mice. **F** Quantification of the percentage of CD4 +T cells in the spleen ($n = 4$ mice/group, one-way ANOVA). **G** Ratio of quantitative percentage of CD4 +T cells to CD8 +T cells in spleen ($n = 4$ mice/group, one-way ANOVA). **H** Elisa analysis of serum IFN-γ concentration ($n = 4$ mice/group, one-way ANOVA). **I** ELISA analysis of IL-10 concentration in serum ($n = 4$ mice/group, one-way ANOVA) ($^{*}P < 0.05$. $^{**}P < 0.01$. $^{***}P < 0.001$)

anti-PD-1 group ($P < 0.01$, $P = 0.002$), and SBRT combined with PD-1 antibody group vs. SBRT group Ki-67 values ($P < 0.01$, $P = 0.003$). The results indicated that the proliferation of tumor cells was attenuated after providing the combination therapy. Immunohistochemical TUNEL was also performed on primary and secondary tumors as shown in Fig. 4D. The immunohistochemical TUNEL was analyzed by ImageJ software, and since the results were consistent with normality and chi-square, a one-way comparative method was used. The OD values of TUNEL for SBRT combined with PD-1 antibody group compared with the control group ($P < 0.001$), the anti-PD-1 group ($P < 0.01$, $P = 0.008$), and the SBRT group ($P < 0.01$, $P = 0.002$) are shown in Fig. 4E. Similarly, Fig. 4F shows the TUNEL OD values for the secondary tumors when SBRT combined with PD-1 antibody was compared with the other groups: vs. control ($P < 0.001$), vs. anti-PD-1

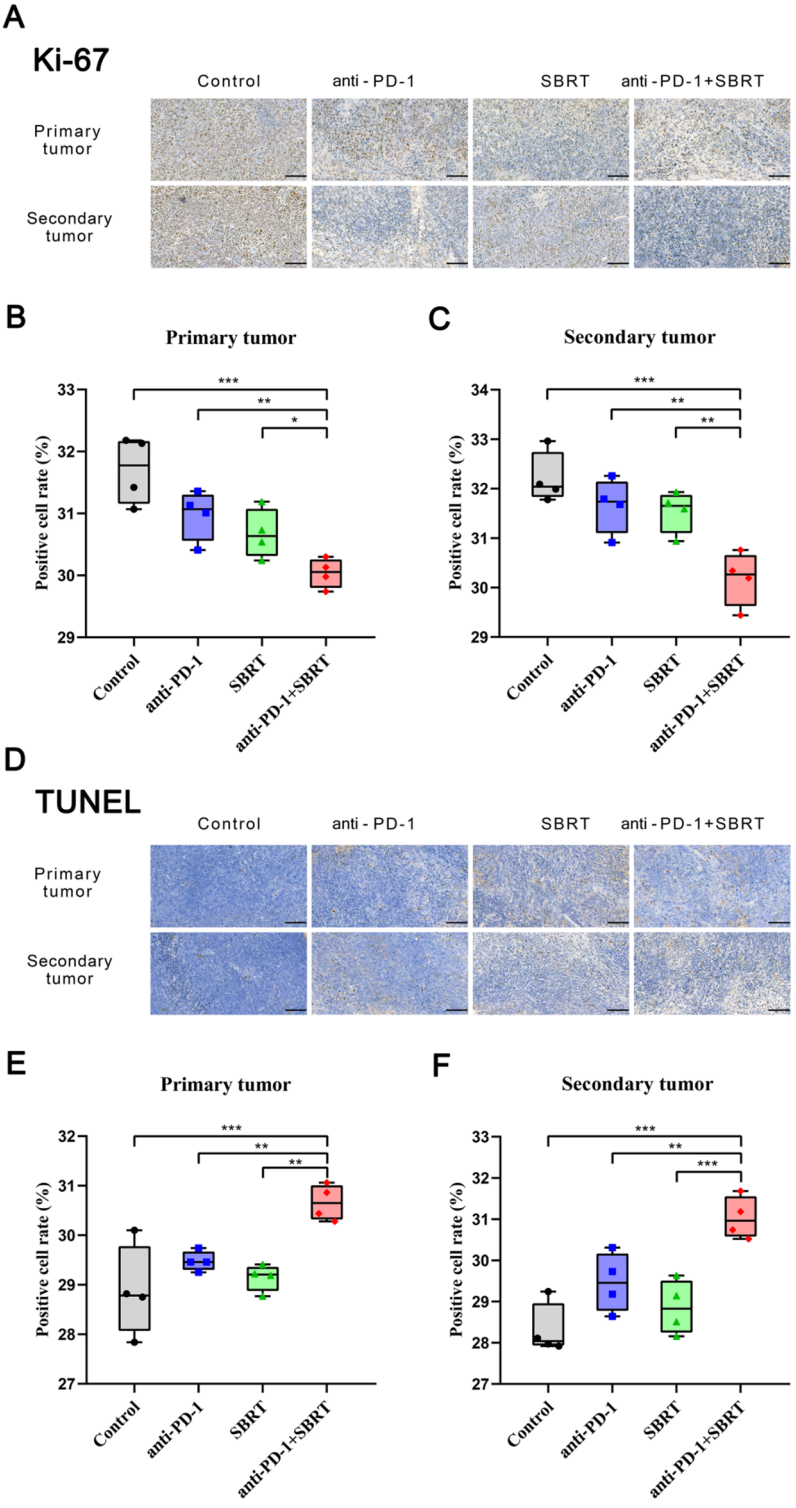

Fig. 4 Tumor cell proliferation is reduced and apoptosis is increased after SBRT combined with PD-1 antibody treatment. **A** Ki-67 staining: brownish yellow for positive proliferating cells, blue for nuclei. **B** Quantitative analysis of Ki-67 expression in primary tumor. **C** Quantitative analysis of Ki-67 expression in secondary tumor. **D** TUNEL paraffin white light staining: brownish yellow corresponds to apoptosis-positive cells, blue represents nuclei. **E** Quantitative analysis of TUNEL expression in primary tumor. **F** Quantitative analysis of TUNEL expression in secondary tumor. (Scale bars: 50 μm). ($^{*}P < 0.05$. $^{**}P < 0.01$. $^{***}P < 0.001$)

group TUNEL OD values ($P < 0.01$, $P = 0.004$) and vs. SBRT group TUNEL OD values ($P < 0.001$). These data suggest that providing treatment with SBRT combined with PD-1 antibody increased apoptosis. In addition, the combined therapy could reduce the proliferation of tumor cells.

3.5 Non-significant toxic side effects of the combination therapy

Figure 5A shows that the treatment did not significantly change the body weight or growth of mice in each group. The liver, spleen, lungs, kidneys, and heart of tumor-bearing mice from each group were stained with hematoxylin-eosin (HE), and the pictures, which were obtained by pathological section scanne, are shown in Fig. 5B. No significant damages were observed in the liver, spleen, lungs, kidneys, and heart cells after the two treatments. Thus, there was no obvious damage to organs or other side effects when combining SBRT with PD-1 antibody treatment, In addition, there was no death in the two combination groups of tumor-bearing mice, indicating good tolerability.

4 Discussion

The median survival time for patients with advanced HCCs is around 6–8 months [32]. Subsequently, those who received sorafenib as a first-line therapy for advanced HCC were found to have 13.6 months median survival [14]. In a phase II metastatic HCC study by Qin S et al., 303 patients were screened between November 15, 2016, and November 16, 2017. Camrelizumab was used in the treatment of 217 of the 220 eligible patients who were randomly allocated (109 patients received treatment every 2 weeks and 108 every 3 weeks). There was a 12 – 5 months (IQR 5.7–15.5) follow-up in this case [33]. In a different phase III study of metastatic HCC by Finn RS et al., the median survival on pembrolizumab was 13.9 months (95% CI, 11.6–16.0) [34]. In our retrospective study, the median survival was 17.5 months, 12.5 months and 5.2 months for the IMRT + anti-PD-1, anti-PD-1 and control respectively. In addition, OS was considerably extended in both IMRT + anti-PD-1 and anti-PD-1 groups compared to the control in both studies. However, the IMRT + anti-PD-1 group had a longer OS than the anti-PD-1 group which was not statistically significant. Our clinical study is consistent with these findings in this regard to immunotherapy monotherapy use. However, because the sample size is too small, the results are biased, and further multicenter research is needed to expand the sample size.

The development of immunotherapy based on ICB has dramatically changed the approach to cancer treatment. This approach elicits durable therapeutic responses and prolongs patient survival. However, not all patients benefit from this approach [35]. Moreover, only a small percentage of patients benefit from single-agent immunotherapies over the long term due to primary and secondary resistance often leads to treatment failure, with only a minority of patients achieving long-term benefits [36]. Most patients that present to the clinic are refractory to anti-PD-1 treatment, or develop resistance over the course of treatment. The effectiveness of immune checkpoint inhibitors is currently limited by low response rates caused by innate or acquired resistance [37]. It has now been well established that by increasing the release and presentation of tumor neoantigens, radiation may drastically change the immunogenicity of TME, and that inflammatory remodeling in the microenvironment after radiation can enhance effector T cell recruitment and activation as well as enhance tumor immunogenicity [23]. The

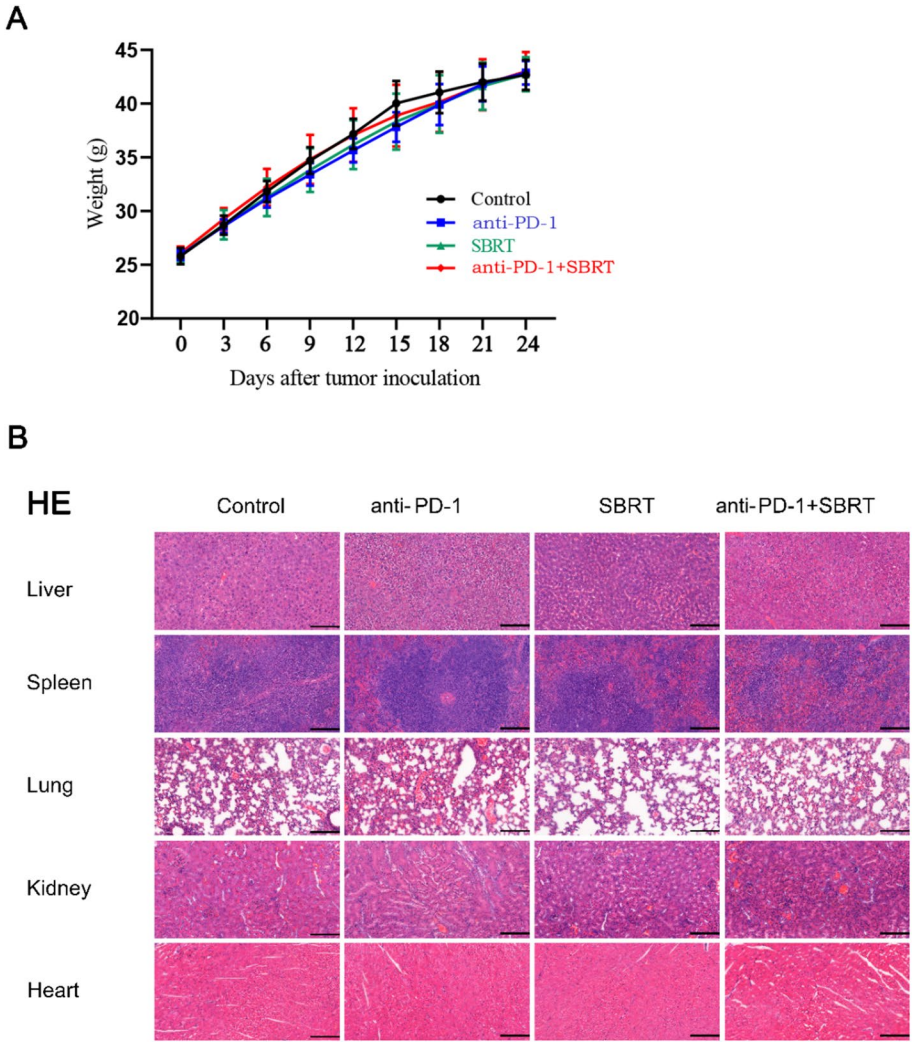

Fig. 5 Toxic side effects of SBRT combined with PD-1 antibody treatment were not obvious in the tumor-bearing mice. **A** Body weight growth curves of each group of tumor-bearing mice ($n = 12$ mice/group, 2-way analysis of variance for body weight growth). **B** Stain plots of H&E of the major organs in different treatment groups. (Scale bar: 50 μm)

preclinical theoretical basis for a combined radiation and ICB approach is the production of immunogenic cell death, increased neoantigen expression and presentation, and CD8 + T cell activation and infiltration [31]. Type I interferons are indeed produced by radiation to induce DC cross-presentation of tumor antigens which subsequently trigger CD8 + effector T cell crossover [38–40]. Type I interferon signaling in tumor cells upregulates multiple T cell suppressor ligands, including anti-PD-1 [41]. Radiotherapy may overcome the drug resistance to anti-PD-1 by changing the tumor microenvironment. In our study in tumor-bearing mice, combination treatment is significantly higher CD8 + effector T cells in primary and secondary tumors. CD4 + T cells and CD4+/CD8 + T cells were also significantly elevated in the spleen. There are studies that show that a combination therapy comprising sorafenib, camrelizumab, TACE, and SBRT is an effective downstaging strategy for advanced HCC with PVTT and is associated with few adverse events [42, 43].

Radiation enhances T cell infiltration and proliferation, thereby increasing the concentration of T cells in tumors [24, 44]. The main effector molecule secreted by tumor infiltrating lymphocytes (TILs) is IFN-γ. IFN-γ has multiple functions that reprogram TIL to become a better effector, which in turn inhibits the growth of tumor cells through the IFNGR1 mechanism [25]. Radiation can also increase the expression of PD-L1 in the tumor microenvironment, which is thought to be associated with the secretion of IFN-γ [31]. In our study, a significantly higher concentration of IFN-γ in the combination treatment group of homozygous mice was analyzed from the serum of mice.

The tumor microenvironment (TME) includes a variety of suppressor immune cells, including Treg cells, macrophages, and MDSCs, as well as other stromal cells.Treg cells secrete the cytokine IL-10 in the tumor microenvironment, and IL-10 inhibits effector T-cell activation [26]. The immunomodulatory mechanism of SBRT and PD-1/PD-L1 inhibitors in anti-tumor immunity reveals a potential synergistic effect of the two in tumor treatment. The combination of SBRT and PD-1/PD-L1 inhibitors not only enhances positive immune regulation, but also significantly reduces negative immune resistance. SBRT has been shown to promote the release of tumor associated antigen, which further induces dendritic cell maturation, cross-sensitization of cytotoxic T lymphocytes, and recruitment of lymphocytes to tumors, thereby transforming immunologically "cold" tumors into "hot" tumors [45]. Recovery of CD8 + T cells after PD-1/PD-L1 inhibitor treatment induces the production of TNFα, which further leads to the elimination of myeloid-derived suppressor cells. Studies have shown that macrofractionated radiotherapy alone cannot produce lasting anti-tumor immunity, but when used in combination with PD-1/PD-L1 inhibitors, it can induce protective immune memory in long-term survivors with increased memory CD8 + T cells [46]. In our study, the concentration of IL-10 in the blood of mice treated with stereotactic body radiation therapy (SBRT) combined with PD-1 antibody was significantly reduced, which reduced immunosuppression and was more favorable for anti-tumor effects.

Radiation dosages used in SBRT have more immunogenic effects than those used in conventional radiation therapy, but these doses may also cause vascular damage and worsen tumor hypoxia. However, anti-PD-1 treatment not only leads to tumor regression but also reduces tumor hypoxia [29]. Evidence suggests that 8 Gy×3 F radiation doses generated immunogenic changes in TME and are more beneficial in promoting T-cell infiltration and the reduction of tumors in the local and distant environment [47]. To further confirm its efficacy in metastatic HCC, animal-based experiments were conducted. For radiotherapy modality, 8 Gy×3 F radiotherapy was selected, and the pd-1 antitumor efficacy was dramatically boosted by the dosage of radiation. But some studies have shown that post low-dose radiotherapy (LDRT) effector immune cells such as T cells and NK cells increase the homing of tumors. LDRT can enhance the activity and persistence of effector T cells needed for successful checkpoint inhibition (CPI) and adoptive cell therapy (ACT) by breaking the matrix barrier and regulating tumor microenvironment (TME) [48, 49]. So, current studies remain inconclusive regarding the radiation dose and modality to obtain the optimal efficacy, and as such, further studies are warranted.

As mentioned above, SBRT significantly enhances the antitumor efficacy of immunotherapy. However, many data suggest that immune-related adverse events (IrAE) may also occur in patients following the use of PD-1 antibodies. The toxicity profile of

immune checkpoint inhibitors (ICIs) differs from that of standard chemotherapy or other biologic agents, with most toxicity arising from over-immunization of normal tissues [50]. Immune checkpoint drugs that target PD-1, PD-L1, and CTLA-4 have seen increased usage in certain cancer treatments in the last several decades because of advancements in cancer immunotherapy [51–53]. However, because of the increasing usage, there have been more reports of IrAE, that tend to be unique. In contrast to conventional cancer therapy, these treatments have delayed onset and extended duration. Furthermore, despite the fact that IrAE may affect any organ or system, they are often low-grade, curable, and reversible. However, some serious side effects may lead to a long-term health problems [54]. In our SBRT combined with PD-1 antibody animal experiments, there was no death in all groups of tumor-bearing mice, no significant difference in body weight growth between the groups of tumor-bearing mice, and there was no organ damage in any of the organs of the liver, spleen, lungs, kidneys, and heart. However, despite the fact that IrAE may affect any organ system, the median onset time depends on the afflicted organ system and can occur anywhere within 2–16 weeks after the therapy begins [55].

Although we demonstrated through clinical studies and animal experiments that SBRT could increase anti-PD-1 activity by enhancing the tumor immune microenvironment in mice, and that no significant adverse effects occurred during the observation period of animal experiments (17 days after starting treatment), there are many limitations of our study. SBRT was used only once in the animal trial, however, in the clinical study, it was used in the liver (lesions < 4, diameter < 5 cm). Secondly, the observation time in the animal study was 17 days, which could represent a too short observation time to reflect the survival advantage of the combination therapy. In addition, the immune drug anti-PD-1 used in patients was not uniform, the sample size was small in each group, the doses of IMRT and SBRT were inconsistent, and the follow-up information of some patients was not available leading to failure to obtain post-treatment safety assessment of patients. Therefore, on the basis of this study, we plan to further study the anti-tumor mechanism of more molecules in the tumor microenvironment and observe the changes of bone marrow cells in the tumor. And further compare the similarities and differences of two different radiotherapy methods of IMRT and SBRT in the mouse model combined with anti-PD-1, and explore the best treatment for patients with metastatic liver cancer. In addition, other anticancer drugs such as Histone Deacetylase (HDAC) inhibitors also showed distinct and beneficial immune-sensitizing effects in solid tumors, which might be considered for future studies [56, 57].

5 Conclusions

This study demonstrated remarkable results showing that SBRT significantly greatly increases anti-PD-1 antitumor activity by enhancing the tumor immune microenvironment in mice with metastatic hepatocellular carcinoma, showing complete cancer cure in half of the mice. This observation could be linked to increased infiltration of CD8 + effector T cells prompted by radiotherapy. Furthermore, no damage to individual organs was observed, and no mortality occurred in the tumor-bearing mice after providing the combination therapy. We studied the toxic and side effects for the first time. This indicates that this treatment modality was effective and well-tolerated, but further validation studies are warranted.

Acknowledgements
Not applicable.

Author contributions
KX, TG, KS, LG, XL, BH, JH, HLL, RX, HC, XT, QY, XCZ, XZ and YL participated in animal experiments. JX, PW and HL collected the data. KX, TG, KS, KH and YH wrote the manuscript and analyzed the data. KH and YH designed the research study. All authors approved the final version of the manuscript.

Funding
This study was supported by the Medical Research Foundation of Chongqing GeneralHospital (Y2023YXYJMSXM04), the Science and Technology Research Program of Chongqing Municipal Education Commission (Grant No.KJQN202400116), the Natural Science Foundation of Sichuan Province (No.2025ZNSFSC1883), the Key Project of Sichuan Science and Technology Program (No. 2022YFS0622-A6), the Program of Sichuan Medical Association (No. S23044), the Applied Basic Research Project of Luzhou Science and Technology and Talent Work Bureau (No. 2022-JYJ-123), the Key Project of Southwest Medical University (No. 2024LCYXZX23), the Strategic Cooperation Project of Luzhou Municipal People's Government-Southwest Medical University (No. 2024LZXNYDJ058), the General Project of Southwest Medical University (No. 2024LCYXZX54), the Program of Affiliated Hospital of Southwest Medical University (No. HYX22009), and the Cultivation Project of Sichuan Computer Research Institute (No. MZGC20240014).

Data availability
All the original data and images can be found in the links below https://www.jianguoyun.com/p/DXJU3FYQ7NLdChjtu8oEIAA.

Declarations

Ethics approval and consent to participate
This trial complied with the Declaration of Helsinki and was approved by the Clinical Trials Ethics Committee of the Affiliated Hospital of Southwest Medical University (Approval No. KY2020254). Due to the retrospective nature of the study, the requirement for informed consent was waived by the Ethics Committee of the Affiliated Hospital of Southwest Medical University. No potentially identifying information or images of human participants are included in this article. All methods were carried out in accordance with relevant guidelines and regulations. The study conforms to the ARIVE guidelines and should be carried out in accordance with the 1964 Declaration of Helsinki and its later amendments or comparable ethical standards, the U.K. Animals (Scientific Procedures) Act, 1986 and associated guidelines(https://www.wma.net/what-we-do/medical-ethics/declaration-of-helsinki/). EU Directive 2010/63/EU for animal experiments, or the National Institutes of Health guide for the care and use of Laboratory animals (NIH Publications No. 8023, revised 1978). The Ethics Committee of Southwest Medical University (SWMU) stipulates that the Ethics Committee allows a tumor load of 2 cm or approximately 10% of the body weight of the mice, and the tumor sizes during tumor modeling of the mice involved in this study were in accordance with the regulations of the Ethics Committee of Southwest Medical University. Animal experiments were carried out in accordance with animal care guidelines and were authorized by the Institutional Animal Care and Treatment Committee of Southwest Medical University (Luzhou, China) (approval No. SWMU20220042).

Competing interests
The authors declare no competing interests.

Author details
[1]Department of Oncology, The Affiliated Hospital, Southwest Medical University, Luzhou 646000, China
[2]Department of Oncology, Chongqing General Hospital, Chongqing 401147, China
[3]Department of Radiation Oncology, National Clinical Research Center for Cancer/Cancer Hospital, National Cancer Center, Chinese Academy of Medical Sciences and Peking Union Medical College, Beijing 100000, China
[4]Clinical Medical College, Southwest Medical University, Luzhou 646000, China
[5]Department of Public Health, Southwest Medical University, Luzhou 646000, China
[6]Clinical Skills Center, The Affiliated Hospital of Southwest Medical University, Luzhou 646000, China
[7]Clinical Research Institute, The Affiliated Hospital of Southwest Medical University, Luzhou 646000, China
[8]Department of Ophthalmology, The Affiliated Hospital of Southwest Medical University, Luzhou 646000, China
[9]Nuclear Medicine and Molecular Imaging Key Laboratory of Sichuan Province, Luzhou 646000, China
[10]Academician (Expert) Workstation of Sichuan Province, Luzhou 646000, China
[11]The Affiliated Hospital of Southwest Medical University, 25 Taiping Street, Luzhou, Sichuan, China

Received: 28 July 2024 / Accepted: 4 June 2025
Published online: 13 June 2025

References

1. Sung H, Ferlay J, Siegel RL, Laversanne M, Soerjomataram I, Jemal A, Bray F. Global Cancer statistics 2020: GLOBOCAN estimates of incidence and mortality worldwide for 36 cancers in 185 countries. Cancer J Clin. 2021;71:209–49.
2. Ghouri YA, Mian I, Rowe JH. Review of hepatocellular carcinoma: epidemiology, etiology, and carcinogenesis. J Carcinog. 2017;16:1.
3. Llovet JM, Kelley RK, Villanueva A, Singal AG, Pikarsky E, Roayaie S, Lencioni R, Koike K, Zucman-Rossi J, Finn RS. Hepatocellular carcinoma. Nat Rev Dis Primers. 2021;7:6.
4. Ginès P, Krag A, Abraldes JG, Solà E, Fabrellas N, Kamath PS. Liver cirrhosis. Lancet (London England). 2021;398:1359–76.
5. O'Rourke JM, Sagar VM, Shah T, Shetty S. Carcinogenesis on the background of liver fibrosis: implications for the management of hepatocellular cancer. World J Gastroenterol. 2018;24:4436–47.

6. Forner A, Reig M, Bruix J. Hepatocellular carcinoma. Lancet (London England). 2018;391:1301–14.
7. Zamora-Valdes D, Taner T, Nagorney DM. Surgical treatment of hepatocellular carcinoma. Cancer Control: J Moffitt Cancer Cent. 2017;24:1073274817729258.
8. Hartke J, Johnson M, Ghabril M. The diagnosis and treatment of hepatocellular carcinoma. Semin Diagn Pathol. 2017;34:153–9.
9. Kudo M. Treatment of advanced hepatocellular carcinoma with emphasis on hepatic arterial infusion chemotherapy and molecular targeted therapy. Liver cancer. 2012;1:62–70.
10. Bouattour M, Mehta N, He AR, Cohen EI, Nault JC. Systemic treatment for advanced hepatocellular carcinoma. Liver cancer. 2019;8:341–58.
11. Bruix J, Raoul JL, Sherman M, Mazzaferro V, Bolondi L, Craxi A, Galle PR, Santoro A, Beaugrand M, Sangiovanni A, Porta C, Gerken G, Marrero JA, Nadel A, Shan M, Moscovici M, Voliotis D, Llovet JM. Efficacy and safety of Sorafenib in patients with advanced hepatocellular carcinoma: subanalyses of a phase III trial. J Hepatol. 2012;57:821–9.
12. Yoo GS, Ahn WG, Kim SY, Kang W, Choi C, Park HC. Radiation-induced abscopal effect and its enhancement by programmed cell death 1 Blockade in the hepatocellular carcinoma: A murine model study. Clin Mol Hepatol. 2021;27:144–56.
13. Forner A, Reig ME, de Lope CR, Bruix J. Current strategy for staging and treatment: the BCLC update and future prospects. Semin Liver Dis. 2010;30:61–74.
14. Kudo M, Finn RS, Qin S, Han KH, Ikeda K, Piscaglia F, Baron A, Park JW, Han G, Jassem J, Blanc JF, Vogel A, Komov D, Evans TRJ, Lopez C, Dutcus C, Guo M, Saito K, Kraljevic S, Tamai T, Ren M, Cheng AL. Lenvatinib versus Sorafenib in first-line treatment of patients with unresectable hepatocellular carcinoma: a randomised phase 3 non-inferiority trial. Lancet (London England). 2018;391:1163–73.
15. Casadei-Gardini A, Scartozzi M, Tada T, Yoo C, Shimose S, Masi G, Lonardi S, Frassineti LG, Nicola S, Piscaglia F, Kumada T, Kim HD, Koga H, Vivaldi C, Soldà C, Hiraoka A, Bang Y, Atsukawa M, Torimura T, Tsuj K, Itobayashi E, Toyoda H, Fukunishi S, Rimassa L, Rimini M, Cascinu S, Cucchetti A. Lenvatinib versus Sorafenib in first-line treatment of unresectable hepatocellular carcinoma: an inverse probability of treatment weighting analysis. Liver Int: Off J Int Assoc Study Liver. 2021;41:1389–97.
16. Zheng Y, Wang S, Cai J, Ke A, Fan J. The progress of immune checkpoint therapy in primary liver cancer. Biochimica et biophysica acta. Reviews cancer. 2021;1876:188638.
17. Lei X, Lei Y, Li JK, Du WX, Li RG, Yang J, Li J, Li F, Tan HB. Immune cells within the tumor microenvironment: biological functions and roles in cancer immunotherapy. Cancer Lett. 2020;470:126–33.
18. Shen Z, Li M, Bai S, Yang Q, Zhang F, Tang M, Guo J, Yang Z. [Progress in immunotherapy for hepatocellular carcinoma]. Sheng Wu Gong Cheng Xue bao = chinese. J Biotechnol. 2019;35:2326–38.
19. Tian M, Shi Y, Liu W, Fan J. Immunotherapy of hepatocellular carcinoma: strategies for combinatorial intervention. Sci China Life Sci. 2019;62:1138–43.
20. Ngwa W, Irabor OC, Schoenfeld JD, Hesser J, Demaria S, Formenti SC. Using immunotherapy to boost the abscopal effect. Nat Rev Cancer. 2018;18:313–22.
21. Rodríguez-Ruiz ME, Vanpouille-Box C, Melero I, Formenti SC, Demaria S. Immunological mechanisms responsible for Radiation-Induced abscopal effect. Trends Immunol. 2018;39:644–55.
22. Postow MA, Callahan MK, Barker CA, Yamada Y, Yuan J, Kitano S, Mu Z, Rasalan T, Adamow M, Ritter E, Sedrak C, Jungbluth AA, Chua R, Yang AS, Roman RA, Rosner S, Benson B, Allison JP, Lesokhin AM, Gnjatic S, Wolchok JD. Immunologic correlates of the abscopal effect in a patient with melanoma. N Engl J Med. 2012;366:925–31.
23. Donlon NE, Power R, Hayes C, Reynolds JV, Lysaght J. Radiotherapy, immunotherapy, and the tumour microenvironment: turning an immunosuppressive milieu into a therapeutic opportunity. Cancer Lett. 2021;502:84–96.
24. Arina A, Beckett M, Fernandez C, Zheng W, Pitroda S, Chmura SJ, Luke JJ, Forde M, Hou Y, Burnette B, Mauceri H, Lowy I, Sims T, Khodarev N, Fu YX, Weichselbaum RR. Tumor-reprogrammed resident T cells resist radiation to control tumors. Nat Commun. 2019;10:3959.
25. Meister N, Shalaby T, von Bueren AO, Rivera P, Patti R, Oehler C, Pruschy M, Grotzer MA. Interferon-gamma mediated up-regulation of caspase-8 sensitizes Medulloblastoma cells to radio- and chemotherapy. Eur J cancer (Oxford England: 1990). 2007;43:1833–41.
26. Weichselbaum RR, Liang H, Deng L, Fu YX. Radiotherapy and immunotherapy: a beneficial liaison? Nature reviews. Clin Oncol. 2017;14:365–79.
27. Choi C, Yoo GS, Cho WK, Park HC. Optimizing radiotherapy with immune checkpoint Blockade in hepatocellular carcinoma. World J Gastroenterol. 2019;25:2416–29.
28. Chen Y, Gao M, Huang Z, Yu J, Meng X. SBRT combined with PD-1/PD-L1 inhibitors in NSCLC treatment: a focus on the mechanisms, advances, and future challenges. J Hematol Oncol. 2020;13:105.
29. Zheng X, Fang Z, Liu X, Deng S, Zhou P, Wang X, Zhang C, Yin R, Hu H, Chen X, Han Y, Zhao Y, Lin SH, Qin S, Wang X, Kim BY, Zhou P, Jiang W, Wu Q, Huang Y. Increased vessel perfusion predicts the efficacy of immune checkpoint Blockade. J Clin Investig. 2018;128:2104–15.
30. Seiwert TY, Kiess AP. Time to debunk an urban myth?? The abscopal effect with radiation and Anti-PD-1. J Clin Oncol: Off J Am Soc Clin Oncol. 2021;39:1–3.
31. Dovedi SJ, Adlard AL, Lipowska-Bhalla G, McKenna C, Jones S, Cheadle EJ, Stratford IJ, Poon E, Morrow M, Stewart R, Jones H, Wilkinson RW, Honeychurch J, Illidge TM. Acquired resistance to fractionated radiotherapy can be overcome by concurrent PD-L1 Blockade. Cancer Res. 2014;74:5458–68.
32. EASL Clinical Practice Guidelines. Management of hepatocellular carcinoma. J Hepatol. 2018;69:182–236.
33. Qin S, Ren Z, Meng Z, Chen Z, Chai X, Xiong J, Bai Y, Yang L, Zhu H, Fang W, Lin X, Chen X, Li E, Wang L, Chen C, Zou J. Camrelizumab in patients with previously treated advanced hepatocellular carcinoma: a multicentre, open-label, parallel-group, randomised, phase 2 trial. Lancet Oncol. 2020;21:571–80.
34. Finn RS, Ryoo BY, Merle P, Kudo M, Bouattour M, Lim HY, Breder V, Edeline J, Chao Y, Ogasawara S, Yau T, Garrido M, Chan SL, Knox J, Daniele B, Ebbinghaus SW, Chen E, Siegel AB, Zhu AX, Cheng AL. Pembrolizumab as Second-Line therapy in patients with advanced hepatocellular carcinoma in KEYNOTE-240: a randomized, double-blind, phase III trial. J Clin Oncol: Off J Am Soc Clin Oncol. 2020;38:193–202.

35. Li JY, Chen YP, Li YQ, Liu N, Ma J. Chemotherapeutic and targeted agents can modulate the tumor microenvironment and increase the efficacy of immune checkpoint Blockades. Mol Cancer. 2021;20:27.
36. Zhu S, Zhang T, Zheng L, Liu H, Song W, Liu D, Li Z, Pan CX. Combination strategies to maximize the benefits of cancer immunotherapy. J Hematol Oncol. 2021;14:156.
37. Haslam A, Prasad V. Estimation of the percentage of US patients with Cancer who are eligible for and respond to checkpoint inhibitor immunotherapy drugs. JAMA Netw Open. 2019;2:e192535.
38. Sun L, Wu J, Du F, Chen X, Chen ZJ. Cyclic GMP-AMP synthase is a cytosolic DNA sensor that activates the type I interferon pathway. Sci (New York N Y). 2013;339:786–91.
39. Marcus A, Mao AJ, Lensink-Vasan M, Wang L, Vance RE, Raulet DH. Tumor-Derived cGAMP triggers a STING-Mediated interferon response in Non-tumor cells to activate the NK cell response. Immunity. 2018;49:754–e7634.
40. Diamond JM, Vanpouille-Box C, Spada S, Rudqvist NP, Chapman JR, Ueberheide BM, Pilones KA, Sarfraz Y, Formenti SC, Demaria S. Exosomes shuttle TREX1-Sensitive IFN-Stimulatory DsDNA from irradiated Cancer cells to DCs. Cancer Immunol Res. 2018;6:910–20.
41. Benci JL, Xu B, Qiu Y, Wu TJ, Dada H, Twyman-Saint Victor C, Cucolo L, Lee DSM, Pauken KE, Huang AC, Gangadhar TC, Amaravadi RK, Schuchter LM, Feldman MD, Ishwaran H, Vonderheide RH, Maity A, Wherry EJ. Minn, tumor interferon signaling regulates a Multigenic resistance program to immune checkpoint Blockade. Cell. 2016;167:1540–e155412.
42. Huang Y, Zhang Z, Liao W, Hu K, Wang Z. Combination of sorafenib, camrelizumab, transcatheter arterial chemoembolization, and stereotactic body radiation therapy as a novel downstaging strategy in advanced hepatocellular carcinoma with portal vein tumor thrombus: A case series study. Front Oncol. 2021;11:650394.
43. Bettinger D, Pinato DJ, Schultheiss M, et al. Stereotactic body radiation therapy as an alternative treatment for patients with hepatocellular carcinoma compared to sorafenib: A propensity score analysis. Liver Cancer. 2019;8(4):281–94.
44. Lugade AA, Moran JP, Gerber SA, Rose RC, Frelinger JG, Lord EM. Local radiation therapy of B16 melanoma tumors increases the generation of tumor antigen-specific effector cells that traffic to the tumor. J Immunol. 2005;174:7516–23.
45. Bernstein MB, Krishnan S, Hodge JW, Chang JY. Immunotherapy and stereotactic ablative radiotherapy (ISABR): a curative approach? Nat Rev Clin Oncol. 2016;13(8):516–24.
46. Deng L, Liang H, Burnette B, et al. Irradiation and anti-PD-L1 treatment synergistically promote antitumor immunity in mice. J Clin Invest. 2014;124(2):687–95.
47. Dewan MZ, Galloway AE, Kawashima N, Dewyngaert JK, Babb JS, Formenti SC, Demaria S. Fractionated but not single-dose radiotherapy induces an immune-mediated abscopal effect when combined with anti-CTLA-4 antibody. Clin Cancer Res: Off J Am Assoc Cancer Res. 2009;15:5379–88.
48. Barsoumian HB, Ramapriyan R, Younes AI, Caetano MS, Menon H, Comeaux NI, Cushman TR, Schoenhals JE, Cadena AP, Reilly TP, Chen D, Masrorpour F, Li A, Hong DS, Diab A, Nguyen QN, Glitza I, Ferrarotto R, Chun SG, Cortez MA, Welsh J. Low-dose radiation treatment enhances systemic antitumor immune responses by overcoming the inhibitory stroma. J Immunother Cancer. 2020;8:e000537.
49. Correia AL, Guimaraes JC, Auf der Maur P, De Silva D, Trefny MP, Okamoto R, Bruno S, Schmidt A, Mertz K, Volkmann K, Terracciano L, Zippelius A, Vetter M, Kurzeder C, Weber WP. Bentires-Alj, hepatic stellate cells suppress NK cell-sustained breast cancer dormancy. Nature. 2021;594:566–71.
50. Postow MA, Sidlow R, Hellmann MD. Immune-Related adverse events associated with immune checkpoint Blockade. N Engl J Med. 2018;378:158–68.
51. Yan J, Sui J. Long-term survival after immunotherapy for uncontrolled locally advanced Temporal bone squamous cell carcinoma followed by chemoradiotherapy: A case report. Prec Radiat Oncol. 2024;8:99–105.
52. Meng K, Lu H. Clinical application of high-LET radiotherapy combined with immunotherapy in malignant tumors. Prec Radiat Oncol. 2024;8:42–6.
53. Nakamura D, Honda K, Yamazaki T, et al. Stereotactic body radiation therapy for clinically diagnosed early-stage non-small cell lung cancer: importance of accurate CT interpretation by experts. Prec Radiat Oncol. 2024;8:30–6.
54. Ramos-Casals M, Brahmer JR, Callahan MK, Flores-Chávez A, Keegan N, Khamashta MA, Lambotte O, Mariette X, Suárez-Almazor PA. Immune-related adverse events of checkpoint inhibitors. Nat Rev Dis Primers. 2020;6:38.
55. Weber JS, D'Angelo SP, Minor D, Hodi FS, Gutzmer R, Neyns B, Hoeller C, Khushalani NI, Miller WH Jr., Lao CD, Linette GP, Thomas L, Lorigan P, Grossmann KF, Hassel JC, Maio M, Sznol M, Ascierto PA, Mohr P, Chmielowski B, Bryce A, Svane IM, Grob JJ, Krackhardt AM, Horak C, Lambert A, Yang AS, Larkin J. Nivolumab versus chemotherapy in patients with advanced melanoma who progressed after anti-CTLA-4 treatment (CheckMate 037): a randomised, controlled, open-label, phase 3 trial. The lancet. Oncology. 2015;16:375–84.
56. Cheng B, Pan W, Xiao Y, et al. HDAC-targeting epigenetic modulators for cancer immunotherapy. Eur J Med Chem. 2024;265:116129.
57. Han R, Nusbaum O, Chen X, Zhu Y. Valeric acid suppresses liver cancer development by acting as a novel HDAC inhibitor. Mol Ther Oncol. 2020;19:8–18.

Publisher's note